Open Access

Research Article

PRNANO

Precis. Nanomed. 2021;4(4):840-850

ANDOVER HOUSE

Characterization of microglial phagocytosis and dendrimer nanoparticle uptake in a neonatal rabbit model of cerebral palsy

Aria C. Shi[1], Elizabeth Smith Khoury[1], Nirnath Sah[1], Amanda Fowler[1], Kevin Liaw[2], Anjali Sharma[2], Rangaramanujam M. Kannan[2,3], Sujatha Kannan[1,4-5] *

[1]*Dept of Anesthesiology and Critical Care Medicine, Johns Hopkins University School of Medicine, Baltimore, MD*
[2]*Center for Nanomedicine, Department of Ophthalmology, Wilmer Eye Institute, Johns Hopkins University School of Medicine, Baltimore, MD*
[3]*Departments of Chemical and Biomolecular Engineering, and Materials Science and Engineering, Johns Hopkins University, Baltimore MD, 21218*
[4]*Kennedy Kreiger Institute, Baltimore, MD 21205*
[5]*Dept of Pediatrics, Johns Hopkins University School of Medicine, Baltimore, MD 21287*

Submitted: September 21, 2021 Accepted: October 26, 2021 Published: October 28, 2021

Graphical Abstract

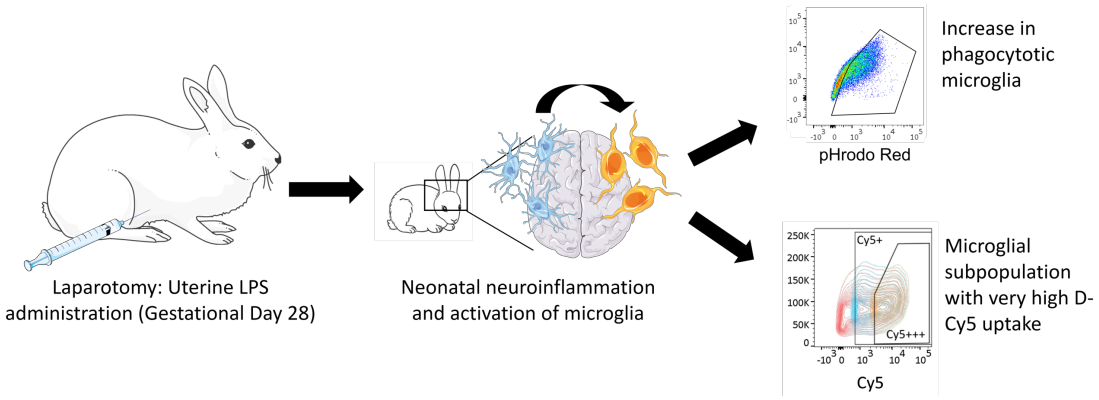

Abstract

Hydroxyl dendrimers target reactive microglia in multiple neuroinflammatory models, including cerebral palsy. Insights on the differential uptake of dendrimers between subpopulations of microglia will enable the better design of precise nanomedicines to treat neuroinflammation. We have previously demonstrated that microglia of rabbits with cerebral palsy undergo change to a pro-inflammatory phenotype that selectively takes up dendrimer nanoparticles proportional to the severity of the injury. However, the functional changes in microglia associated with this activated phenotype and related mechanisms of dendrimer uptake are not well understood. Here, we established a method for isolating microglia from cerebral palsy and healthy neonatal rabbit brains and assessed microglial (1) phagocytic activity ex vivo using fluorescent *E. coli* bioparticles and (2) dendrimer uptake in vivo after intravenous administration of dendrimer conjugated with a fluorescent dye (D-Cy5). Flow cytometry studies showed that the surface marker CD11b is reliably expressed and could isolate microglia from rabbit brain tissue. Furthermore, a significantly higher proportion of microglia isolated from cerebral palsy rabbits demonstrated increased phagocytosis when compared to controls. To assess differences in dendrimer uptake, microglia were isolated from the brain 24 hours after D-Cy5 administration. D-Cy5 localized only in CD11b+ microglia with differential uptake in subpopulations of microglia and was significantly higher in microglia from cerebral palsy rabbits when compared to healthy controls. This study demonstrates that PAMAM hydroxyl dendrimers are preferentially taken up by microglia, especially in cerebral palsy rabbits, and that subpopulations of microglia demonstrate differential dendrimer uptake. Future work will continue to evaluate these subpopulations of microglia further to facilitate the design of precise nanotherapeutics for targeting specific profiles of microglial activation.

* Corresponding author: Prof. S. Kannan, Anesthesiology and Critical Care Medicine & Pediatrics, Johns Hopkins University, Baltimore, MD, skannan3@jhmi.edu

Keywords: PAMAM dendrimer; activated microglia; phagocytosis; neuroinflammation; cerebral palsy

Purpose and Rationale & Introduction

Microglia are major contributors to neuroinflammation and resultant brain injury in cerebral palsy (CP) [1,2]. We have previously shown that *in utero* exposure to lipopolysaccharide (LPS) results in a CP-like phenotype in newborn rabbit kits (e.g., hindlimb hypertonia) along with microglial activation and pro-inflammatory cytokine release [3–5]. We have also demonstrated that systemically-administered hydroxyl polyamidoamine (PAMAM-OH) dendrimers are rapidly excreted by the kidneys and preferentially taken up in 'activated' microglia in the brain of rabbits with CP [6–8]. This allows for targeted delivery of anti-inflammatory payloads such as N-acetylcysteine to modulate microglia 'activation' and dampen subsequent neuroinflammatory damage [8]. It is now well understood that there are multiple states of "activation" of microglia and that these states are often dynamic [9,10]. Less is understood about microglial functional changes (e.g., phagocytosis, endocytosis) and their correlations with CP pathology and dendrimer uptake. Here we explore phagocytosis and dendrimer uptake in microglia in this model to further investigate microglial functionality in perinatal neuroinflammation, which is crucial for developing effective microglial-targeted precision nanotherapeutics.

Materials and Methods

Synthesis of Cy5-labeled PAMAM-OH dendrimer (D-Cy5): D-Cy5 was synthesized using published protocols [7,11]. Briefly, a bifunctional dendrimer is synthesized by partially reacting the hydroxyl groups on PAMAM-OH with BOC-GABA-OH, followed by the BOC deprotection to get amines. The amines are further reacted with Cy5-mono-NHS ester to obtain D-Cy5, characterized using proton nuclear magnetic resonance and high-performance liquid chromatography for structure and purity.

Endotoxin exposure model of CP: All procedures were approved by the Animal Care and Use Committee at Johns Hopkins University. Pregnant New Zealand rabbits (Robinson Services, NC) underwent laparotomy at gestational day (G)28 to inject *Escherichia coli* lipopolysaccharide (LPS) (800-2400 EU) along the uterus. CP kits were delivered on G30. Healthy kits were spontaneously delivered from naïve dams.

Primary Glial Culture: Newborn kit brains were dissociated in 0.05% trypsin (37°C,10 min) as previously described [6], filtered, and cells resuspended in Dulbecco's Modified Eagle's Medium (DMEM) with 10% heat-inactivated fetal bovine serum and 1% penicillin/streptomycin. Cells were plated into poly-L-lysine hydrobromide-coated culture flasks, incubated (37°C, 5% CO_2), and grown to 90% confluence.

Microglia Markers Validation: Primary glial cells were suspended (4×10^5 cells) in a 96-well plate. Cells were stained with Live/dead stain (1:1000 in PBS, 30 min 4°C), incubated in Fc Receptor Binding Inhibitor (1:50 in flow cytometry staining buffer, 10 min, room temperature), stained with fluorescently-conjugated antibodies for CD11b (1:100, 1 h, 4°C) and/or Tomato Lectin (1:150, 1 h, 4°C), fixed with IC Fixation buffer (20 min, room temperature), and washed (Permeabilization Buffer). Cells were then sequentially incubated in anti-Iba1 (1:200 in Permeabilization Buffer, 20 min, room temperature) and donkey anti-goat antibody (1:100, 1 h, 4°C). Flow cytometry was conducted immediately (50,000 events per sample) and analyzed with FlowJo software (complete materials information is listed in the supplement).

Phagocytosis Assay: On postnatal day (PND) 1-7 rabbit kits brains were extracted, minced, incubated in accutase (30 min, 25C, protected from light), and the resulting suspension was filtered and centrifuged (300 g, 10 min, 4°C). After debris removal, microglia were isolated using anti-CD11b microbeads. CD11b+ cells (≥ 200,000) were extracted, suspended in DMEM, and acclimated in the incubator for 24 h. Next, cells were incubated for 1 h in 1:100 pHrodo E.coli Bioparticle for Phagocytosis in DMEM, stained with Live/Dead stain, and fixed with 2% formalin. Finally, cells were resuspended, and flow cytometry was conducted to detect pHrodo fluorescence with ≥ 30,000 events recorded per sample.

D-Cy5 in CD11b+ cells: Kits (PND0-1) were dosed with 55mg/kg of D-Cy5 (containing ~1 mg/kg of Cy5 and corresponds with dendrimer

dose used for efficacy studies) [7, 8] (IV, superficial abdominal vein), sacrificed 24 h later, perfused, and brains collected. The dendrimer dose CD11b+ fractions were collected as described above. Fluorescence-activated cell sorting (FACS) was conducted to quantify Cy5+ cells. This dose was chosen because it is the equivalent dendrimer dose as our preclinical therapeutics using small molecule drugs [8].

Immunohistochemical quantification of D-Cy5: D-Cy5 injected kits were perfused, and brains were collected for subsequent immunostaining [12]. Confocal images of two CP brains (four samplings) and one healthy control brain (three samplings) were acquired and analyzed using ImageJ Analyze Particles function.

Statistics: Data were analyzed using analysis of variance or t-test using Microsoft Excel. Statistics are reported as mean ± standard error.

Results

CD11b is reliably expressed on rabbit microglia

Murine microglia markers CD11b and Lectin were tested as surface markers of rabbit microglia for live-cell acquisition/assessment [13,14]. Co-staining of each marker with Iba1 (rabbit cytosolic microglial marker) was conducted on primary mixed glial cultures. CD11b showed better overlap with Iba1 than did Lectin (Figure 1A).

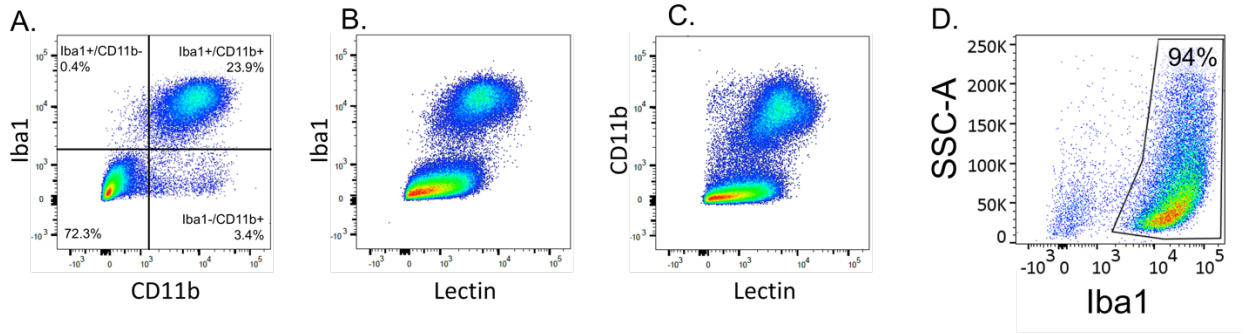

Figure 1. CD11b expression is reliably expressed by rabbit microglia. Known murine microglia markers CD11b, Iba1, and Lectin were explored as methods for isolating the microglia cell population of interest from rabbit brains. Co-staining of two markers were done on primary mixed glial cultures (A-C) and evaluated for overlap. Surface marker CD11b was found to be reliably expressed on rabbit microglia and could be used to isolate microglia from rabbit brain tissue. (D) CD11b+ selection was conducted on two healthy control rabbit brains and stained for Iba1. 94% of the CD11b+ fraction is Iba1+ (n=2, average of two biological replicates). Gating strategies are shown in Supplemental Figure 1.

When co-stained for Iba1 and CD11b, an average of 23.9% of cells of all glial cells present in the culture were Iba1+/CD11b+, 0.4% were Iba1+/CD11b-, and 3.4% were Iba1-/CD11b+. When co-stained for Iba1 and Lectin, cells from Iba1+ and Iba1- populations were variably Lectin+ or Lectin- (Figure 1B). Further, a subpopulation of cells was Lectin+/CD11b-, pointing to a lack of specificity of Lectin (Figure 1C). Thus, CD11b was chosen for subsequent live-cell microglial identification. After bead enrichment, the CD11b+ fraction was 94.0% Iba1+ (n=2; Figure 1D), confirming that the CD11b positive selection successfully isolated microglia, indicating CD11b bead isolation was a reliable method to isolate microglia from the brain.

CP rabbits have a higher proportion of phagocytic microglia

Microglia were isolated from PND1-2 healthy and CP kits and incubated with fluorescent *E. coli* bioparticles and quantified by flow cytometry (Figure 2A-C).

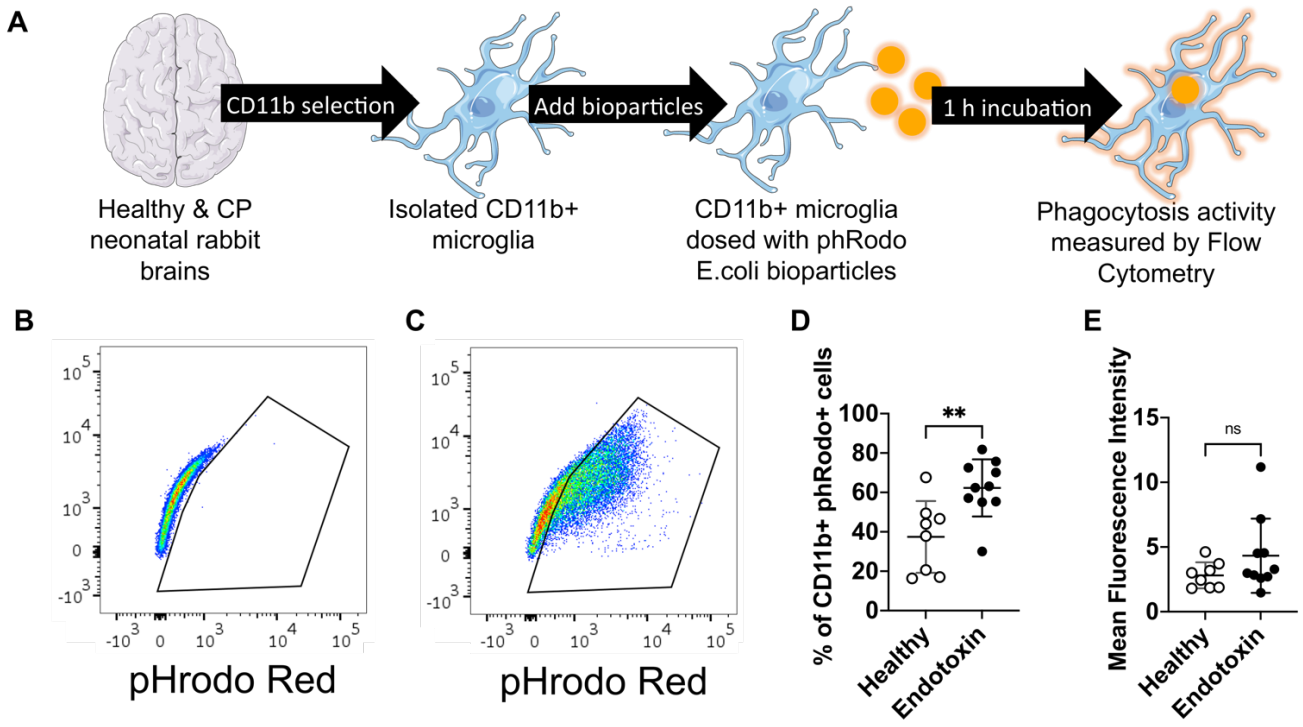

*Figure 2. CP rabbits have a higher proportion of phagocytic microglia than healthy counterparts. A. CD11b+ microglia were incubated with fluorescently labelled E. coli bioparticles for 1 h, and subsequent cell fluorescence was measured by flow cytometry, reflecting the level of phagocytosis activity. B. Gating for fluorescence was determined by examining control cells not exposed to E.coli bioparticles. C. Example data from cells exposed to E.coli bioparticles. D. A significantly higher proportion of microglia (CD11b+) from CP brains were phagocytic (E.coli+) compared to proportions in healthy controls. E. When endotoxin rabbits are broken down by phenotype severity, there is no relationship between severity and the percentage of E.coli+ microglia. There was no difference in the mean fluorescence intensity between endotoxin and healthy controls, indicating that the number of bioparticles each microglia phagocytosed was not significantly different between groups. ** $p < 0.01$, ns = non-significant*

CP microglia displayed a higher proportion of CD11b+ cells containing E.coli bioparticles (62.3 ± 14.5%, n = 10) versus healthy microglia (42.4 ± 18.2%, n=8; *t*-test $p < 0.01$; Figure 2D). The mean fluorescence intensities of the E.coli+ microglia were not different between groups ($p = 0.217$; Figure 2E).

D-Cy5 localizes to a greater extent in microglia from CP rabbits

CD11b+ (microglia) and CD11b- cells (other non-microglial cells from the brain) were isolated from rabbit brain tissue 24 h after IV D-Cy5 injection on PND1 (Figure 3A). Uptake (as measured by D-Cy5+) was significantly greater in CD11b+ cells (63.8 ± 13.2%) than CD11b- cells (0.59 ± 0.21%, n = 5; $p < 0.0001$, Figure 3B,C), indicating that dendrimer is preferentially taken up by microglia. Dendrimer uptake was also greater in CP microglia than in healthy microglia ($p < 0.0001$; normalized to healthy microglia average, 3D). A subpopulation of microglia was found to have much stronger fluorescence (denoted as D-Cy5+++; Figure 3E and F). CP rabbits had ~90% higher proportion of Cy5+++ microglia than healthy controls ($p = 0.0006$) (Figure 3G).

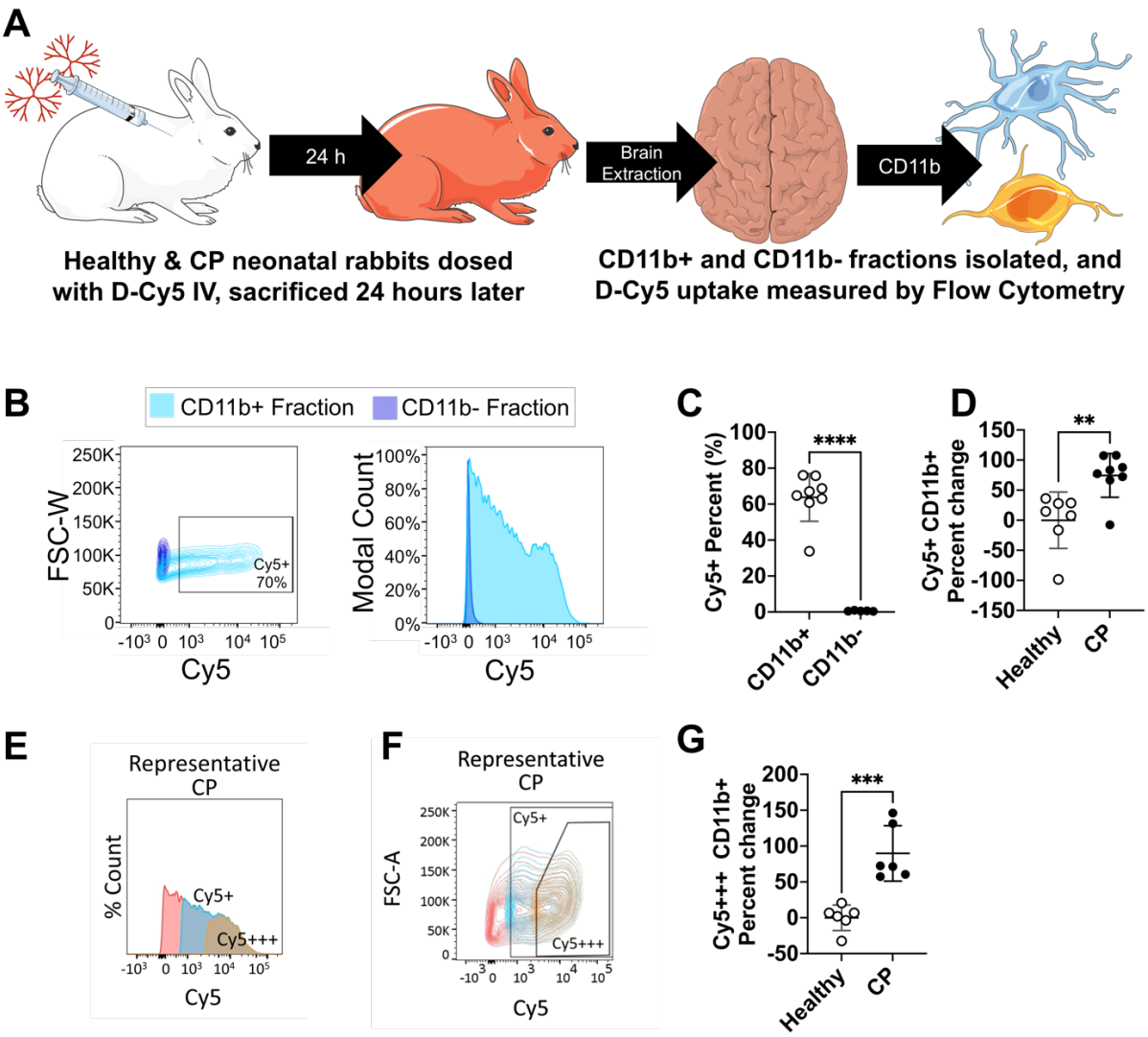

*Figure 3. D-Cy5 is localized to a subset of CD11b+ cells. Fluorescently tagged dendrimers (D-Cy5) were injected IV into neonatal rabbits. Brain tissue was isolated 24 h later, and anti-CD11b microbead enrichment was used to isolate microglia. (A) Flow cytometry then quantified the amount of dendrimer uptake by measuring Cy5 fluorescence in CD11b+ fraction. (B) After anti-CD11b microbead enrichment, Cy5 signal was measured in both CD11b+ (cyan) and CD11b- (violet) fractions. Intravenously dosed D-Cy5 nanoparticles were found in a subset of cells within the CD11b+ fraction but not in the CD11b- fraction. (C) 63% of CD11b+ cells were D-Cy5+ while less than 1% of CD11b- cells were D-Cy5 in CP rabbits. (D) The percent change of Cy5+ microglia in CP kits is significantly greater in relation to Cy5+ microglia from healthy rabbits (E) A subpopulation of CD11b+ Cy5+ microglial cells had distinctly more fluorescence, denoted as Cy5. (F) Density plot also demonstrates two subpopulations of Cy5+ microglia. (G) Cy5+++ microglia were also significantly greater in CP in relation to Cy5+++ healthy microglia in CP rabbit microglia *** $p < 0.001$ compared to healthy control.*

Immunohistochemistry also demonstrated differential uptake within microglial populations. D-Cy5 fluorescence was ensured to be intracellular (Figure 4A and B), and the intensity was observed to be variable across Iba1+Cy5+ cells (Figure 4C and D), implying differential uptake across the microglial population. The histogram plot of normalized D-Cy5 intensity from 851 CP microglia was approximated by three Gaussian curves implying distinct microglial populations with varying levels of cytoplasmic dendrimer (Figure 4D).

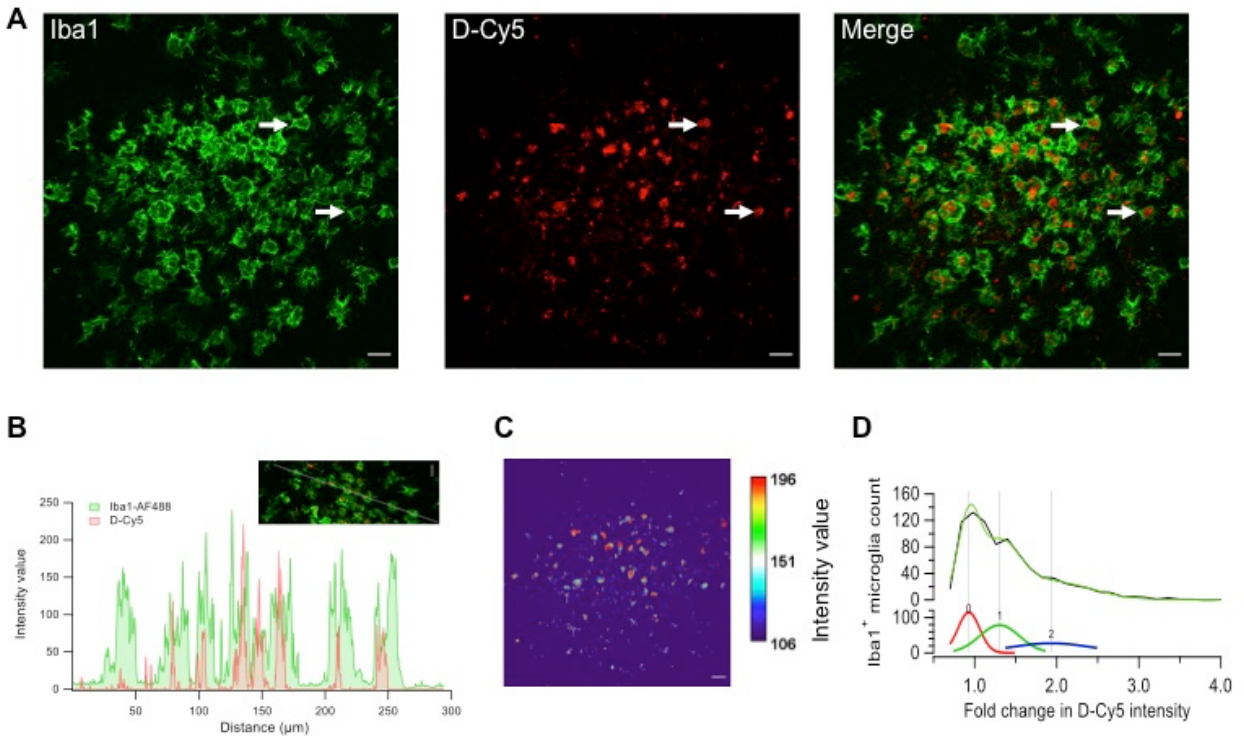

Figure 4. Internalized D-Cy5 signal varies in periventricular microglia. CP rabbit kits injected intravenously with D-Cy5 (10mg/kg) show dendrimer accumulation in activated microglia. (A) Representative confocal images of Iba1+ microglia (green) from white matter show colocalization with dendrimer conjugated with Cy5 (red). Arrows show examples of microglia with internalized dendrimer. Scale bars = 20 μm. (B) A colocalization profile analyzed along cross-section (inset figure) of green (Iba1+ microglia) and red (dendrimer-Cy5) color intensities indicate a significant overlap with multiple peaks of dendrimer and Iba1 intensities. (C) Heat map of D-Cy5 intensity from the representative image shown in (A). (D) The ratio of D-Cy5 intensity of CP microglia to median healthy microglia D-Cy5 intensity is depicted as a histogram plot (top panel, black trace). The histogram of 851 CP microglia was fitted with a multi-gaussian function as a sum of several Gaussian distributions (top panel, green trace). Three distinct gaussian populations labeled as "0" (red trace), "1" (green trace) and "2" (blue trace) were detected (bottom panel). While "0" gaussian population represents the microglia with baseline background Cy5 fluorescence, "1" and "2" gaussian populations imply unique microglial populations with increasing dendrimer uptake. The results demonstrated here are from 851 cells analyzed from 7 sections across 2 CP kits and 351 cells analyzed across 3 sections in one age-matched healthy control kit.

Discussion

Here we established CD11b as a reliable marker of rabbit microglia, congruent with Iba1 expression. CD11b expression increases with inflammation and regulates phagocytosis behavior making it particularly relevant for studying microglial functionality in states of inflammation [5,15,16]. CD11b+ microglia from CP kits are more phagocytic compared to healthy counterparts. Previously we have also shown that CP microglia have decreased migration distance and velocity [1, 17–19]. Increased phagocytosis suggests that decreased migration may be beneficial, and microglia remain to phagocytose in cell debris areas. Interestingly, the phagocytosis of each phagocytosing microglia was similar between endotoxin and healthy samples, but disease severity causes an increase in the percentage of phagocytic microglia.

D-Cy5 was found to localize to a greater extent in a subset of CD11b+ microglia in FACS and immunohistochemical preparations. Previously we have observed that dendrimer rapidly accumulates in the kidney and is excreted through the urine, with minimal uptake in other organs, and is selectively taken up by activated microglia in the brain. The degree of uptake correlates with disease severity [7, 20,21]. Using FACS, we observed a small proportion of healthy microglia positive for Cy5, which may be due to uptake in vessel-associated microglia or perivascular macrophages [22]. We also found a subpopulation of

microglia that shows much higher D-Cy5 positivity; this subpopulation is significantly larger in CP versus healthy kits. Because microglia were isolated from the whole brain tissue, including areas with significant neuroinflammation (i.e., periventricular region) and areas without[5], the observed variable dendrimer uptake may reflect different microglial populations with functional differences between subpopulations. D-Cy5 uptake may be due to heterogeneous microglial profiles [10,23] and differences in other cell uptake processes such as endocytosis and pinocytosis, mechanisms by which dendrimer uptake has been shown to occur [6,24,25].

While both dendrimer uptake and phagocytosis increase in CP microglia, primary uptake of dendrimer is likely not via phagocytosis, as the uptake mechanism is heavily dependent on particle size. Phagocytosis functions optimally with particles approximately 1-3 μm (e.g., the size of E. coli) [26]. Dendrimers and other nano-scale particles may be taken up through clathrin-independent fluid-phase endocytosis and other mechanisms upregulated in activated microglia such as aquaporin channels or receptor-mediated uptake [6,24,27].

Conclusions

This study demonstrates that hydroxyl terminated PAMAM dendrimers are preferentially taken up by activated microglia involved in neuroinflammation. However, subpopulations of microglia demonstrate differential dendrimer uptake. Future studies will focus on defining microglial functional differences that dictate dendrimer nanoparticle uptake after injury and therapy. Identification of cellular subpopulations and their interactions with nanoparticles is crucial for advancing dendrimer therapeutics for precision nanomedicine and will enable more precise targeting and manipulation to modulate the therapeutic response.

Acknowledgments:

This work is supported in part by R01NS093416 and U01NS103882 (SK, RMK).

Conflict of interest

The authors (RMK, SK) have awarded and pending patents relating to hydroxyl dendrimer targeting of reactive microglia. AS is a co-inventor on pending patents related to this technology. Under license agreements involving Ashvattha Therapeutics Inc. and Johns Hopkins University, Drs. Rangaramanujam, Kannan and the University are entitled to royalty distributions related to this technology. Drs. Rangaramanujam and Kannan are co-founders and hold equity in Ashvattha Therapeutics Inc., a startup, undertaking the clinical translation of dendrimer drug delivery platform. The COI is managed by Johns Hopkins University. For a signed statement, please contact the journal office at editor@precisionnanomedicine.com

Quote this article as Shi AC, Khoury ES, Sah N, Fowler A, Liaw K, Sharma A, Kannan RM, Kannan S, Characterization of microglial phagocytosis and dendrimer nanoparticle uptake in a neonatal rabbit model of cerebral palsy, Precis. Nanomed. 2021;4(4):840-850, https://doi.org/10.33218/001c.29729

References

1. MacLennan AH, Thompson SC, Gecz J. Cerebral palsy: Causes, pathways, and the role of genetic variants. Am. J. Obstet. Gynecol. Elsevier Inc.; 2015;213:779–88.
2. Burd I, Balakrishnan B, Kannan S. Models of Fetal Brain Injury, Intrauterine Inflammation, and Preterm Birth. Am. J. Reprod. Immunol. 2012;67:287–94.
3. Kannan S, Saadani-Makki F, Muzik O, Chakraborty P, Mangner TJ, Janisse J, et al. Microglial activation in perinatal rabbit brain induced by intrauterine inflammation: detection with 11C-(R)-PK11195 and small-animal PET. J. Nucl. Med. 2007;48:946–54.
4. Saadani-makki F, Kannan S, Lu X, Janisse J, Dawe E, Edwin S, et al. Intrauterine administration of endotoxin leads to motor deficits in a rabbit model: a link between prenatal infection and cerebral palsy. Am. J. Obstet. Gynecol. 2010;199:651.e1-651.e7.

5. Zhang Z, Jyoti A, Balakrishnan B, Williams M, Singh S, Chugani DC, et al. Trajectory of inflammatory and microglial activation markers in the postnatal rabbit brain following intrauterine endotoxin exposure. Neurobiol. Dis. Elsevier; 2018;111:153–62.
6. Alnasser Y, Kambhampati SP, Nance E, Rajbhandari L, Shrestha S, Venkatesan A, et al. Preferential and Increased Uptake of Hydroxyl-Terminated PAMAM Dendrimers by Activated Microglia in Rabbit Brain Mixed Glial Culture. Molecules. 2018;23.
7. Lesniak WG, Mishra MK, Jyoti A, Balakrishnan B, Zhang F, Nance E, et al. Biodistribution of fluorescently labeled PAMAM dendrimers in neonatal rabbits: Effect of neuroinflammation. Mol. Pharm. 2013;10:4560–71.
8. Kannan S, Dai H, Navath RS, Balakrishnan B, Jyoti a., Janisse J, et al. Dendrimer-Based Postnatal Therapy for Neuroinflammation and Cerebral Palsy in a Rabbit Model. Sci. Transl. Med. 2012;4:130ra46-130ra46.
9. Dubbelaar ML, Kracht L, Eggen BJL, Boddeke EWGM. The Kaleidoscope of Microglial Phenotypes. Front. Immunol. 2018;9:1753.
10. Sousa C, Golebiewska A, Poovathingal SK, Kaoma T, Pires‐Afonso Y, Martina S, et al. Single‐cell transcriptomics reveals distinct inflammation‐induced microglia signatures. EMBO Rep. 2018;19:1–17.
11. Sharma A, Liaw K, Sharma R, Zhang Z, Kannan S, Kannan RM. Targeting mitochondrial dysfunction and oxidative stress in activated microglia using dendrimer-based therapeutics. Theranostics. 2018;8:5529–47.
12. Zhang Z, Saraswati M, Koehler RC, Robertson C, Kannan S. A New Rabbit Model of Pediatric Traumatic Brain Injury. J. Neurotrauma. 2015;32:1369–79.
13. Amici SA, Dong J, Guerau-de-Arellano M. Molecular mechanisms modulating the phenotype of macrophages and microglia. Front. Immunol. 2017;8:1–18.
14. Boche D, Perry VH, Nicoll JAR. Review: Activation patterns of microglia and their identification in the human brain. Neuropathol. Appl. Neurobiol. 2013;39:3–18.
15. Chhor V, Moretti R, Le Charpentier T, Sigaut S, Lebon S, Schwendimann L, et al. Role of microglia in a mouse model of paediatric traumatic brain injury. Brain. Behav. Immun. The Author(s); 2017;63:197–209.
16. Brown EJ. Complement receptors and phagocytosis. Curr. Opin. Immunol. 1991;3:76–82.
17. Zhang F, Nance E, Alnasser Y, Kannan R, Kannan S. Microglial migration and interactions with dendrimer nanoparticles are altered in the presence of neuroinflammation. J. Neuroinflammation. Journal of Neuroinflammation; 2016;13:65.
18. Orr AG, Orr AL, Li X-J, Gross RE, Traynelis SF, Neurosci N. Adenosine A 2A receptor mediates microglial process retraction HHS Public Access Author manuscript. Nat Neurosci. 2009;12:872–8.
19. De Simone R, Niturad CE, De Nuccio C, Ajmone-Cat MA, Visentin S, Minghetti L. TGF-ß and LPS modulate ADP-induced migration of microglial cells through P2Y1 and P2Y12 receptor expression. J. Neurochem. 2010;115:450–9.
20. Mishra MK, Beaty CA, Lesniak WG, Kambhampati SP, Zhang F, Wilson MA, et al. Dendrimer Brain Uptake and Targeted Therapy for Brain Injury in a Large Animal Model of Hypothermic Circulatory Arrest. *ACS Nano* 2014; 8 (3): 2134-2147
21. Nance E, Zhang F, Mishra MK, Zhang Z, Kambhampati SP, Kannan RM, et al. Nanoscale effects in dendrimer-mediated targeting of neuroinflammation. Biomaterials. Elsevier Ltd; 2016;101:96–107.
22. Haruwaka K, Ikegami A, Tachibana Y, Ohno N, Konishi H, Hashimoto A, et al. Dual microglia effects on blood brain barrier permeability induced by systemic inflammation. Nat. Commun. Springer US; 2019;10:1–17.
23. Sivagnanam V, Zhu X, Schlichter LC. Dominance of E. coli phagocytosis over LPS in the inflammatory response of microglia. J. Neuroimmunol. Elsevier BV; 2010;227:111–9.
24. Perumal OP, Inapagolla R, Kannan S, Kannan RM. The effect of surface functionality on cellular trafficking of dendrimers. Biomaterials. 2008;29:3469–76.

25. Zhang J, Liu D, Zhang M, Sun Y, Zhang X, Guan G, et al. The cellular uptake mechanism, intracellular transportation, and exocytosis of polyamidoamine dendrimers in multidrug-resistant breast cancer cells. Int. J. Nanomedicine. 2016;11:3677–90.
26. Baranov M V., Kumar M, Sacanna S, Thutupalli S, van den Bogaart G. Modulation of Immune Responses by Particle Size and Shape. Front. Immunol. 2021;11:1–23.
27. Kitchens KM, Kolhatkar RB, Swaan PW, Ghandehari H. Endocytosis inhibitors prevent poly(amidoamine) dendrimer internalization and permeability across caco-2 cells. Mol. Pharm. 2008;5:364–9.

Supporting information

Supplemental Figures

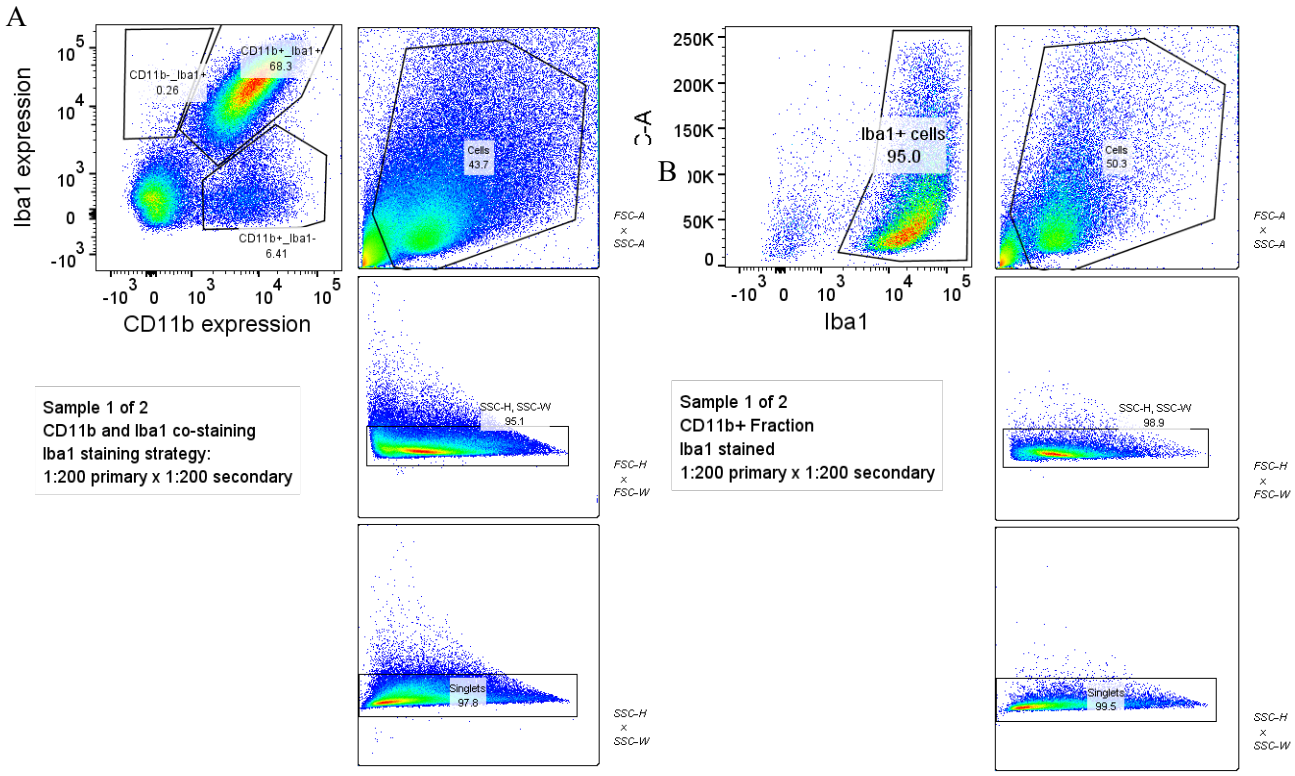

Supplemental Fig 1. Gating strategies for CD11b and Iba1 co-expression, displayed in Figure 1. (A) Rabbit kit brains (n=2) were dissociated, co-stained with Iba1 and CD11b antibodies, and results were visualized by flow cytometry. Clear populations of CD11b+/Iba1+, CD11b+/Iba1-, and Cd11b-/Iba1- cells were found and gated separately. Only a small percentage of CD11b-/Iba1+ cells were found, showing there is good overlap between CD11b and Iba1 staining. (B) Rabbit kit brains (n=2) were dissociated, fractionated using CD11b magnetic beads into CD11b+ and CD11b- fractions. The CD11b+ fraction was stained with Iba1 and results were visualized by flow cytometry. An average of 94% of the CD11b+ fraction stained Iba1+, showing that the CD11b magnetic bead system successfully isolates our cell population of interest.

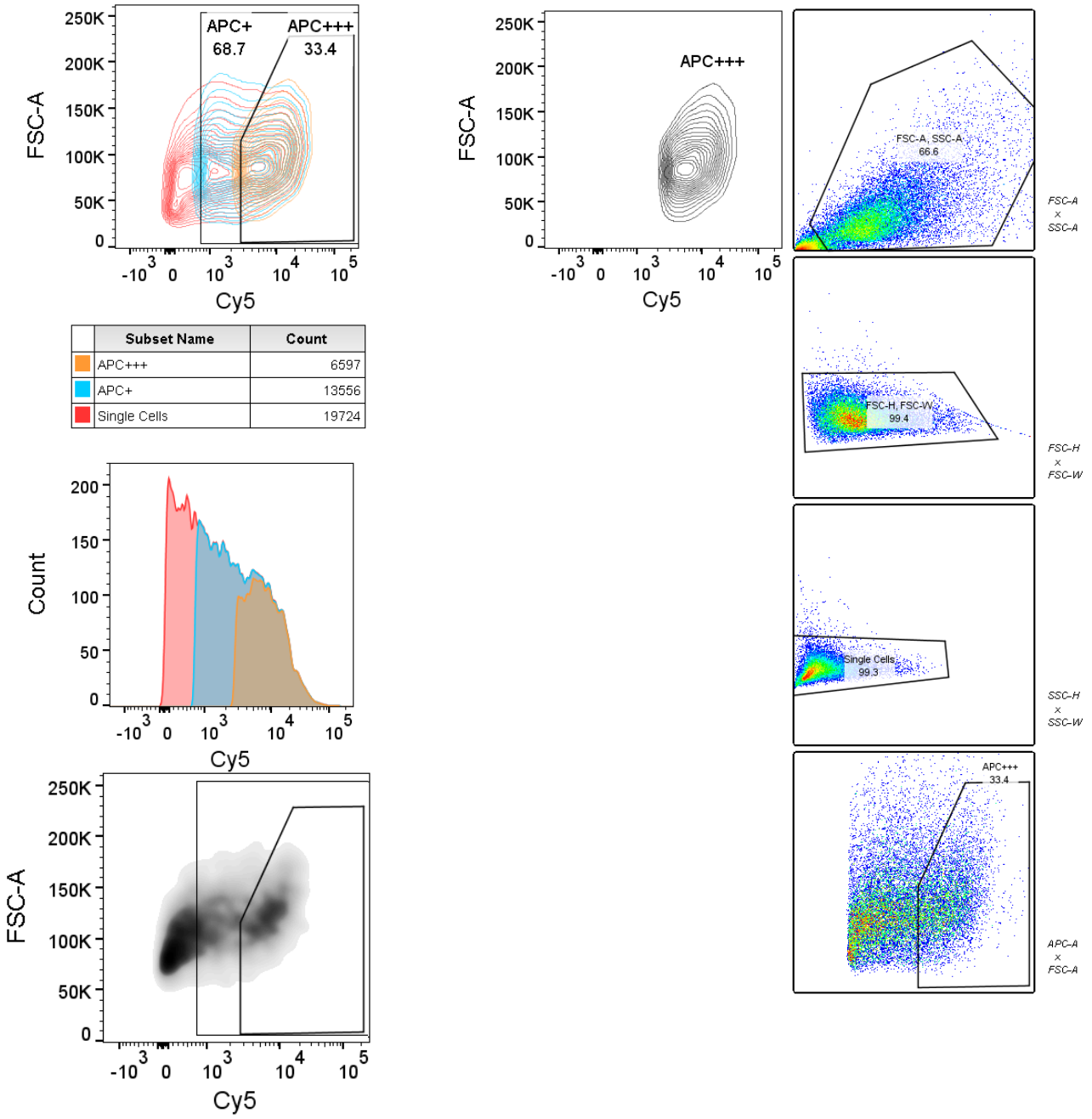

Supplemental Fig 2. Gating strategy for Cy5+ and Cy5+++ fractions, displayed in Figure 3. This is a representative example from a CP rabbit. Neonatal rabbits received systemic IV injection of D-Cy5 and sacrificed 24 hours later. Brains were dissociated and CD11b+ fractions collected. Flow cytometry was conducted to measure Cy5 expression (seen on the APC channel). Cy5+ cells (denoted APC+ in these graphs) were gated by comparing to non-D-Cy5-injected controls. Cy5+++ cells (denoted APC+++ in these graphs) were gated as a freestanding population, best seen in the density plot.

Materials

Item	Product number	Details	Company	Location
New Zealand white rabbits (female)	n/a		Robinson Services Inc.	Winston-Salem, NC, USA
Escherichia coli lipopolysaccharide	L4516	serotype 0127: B8	Sigma Aldrich	St Louis, MO, USA
Dulbecco's Modified Eagle's Medium	21063045		Gibco, ThermoFisher	Carlsbad, CA, USA
10% heat inactivated fetal bovine serum	10082147		Gibco, ThermoFisher	Carlsbad, CA, USA
1% penicillin/streptomycin	15070063		Gibco, ThermoFisher	Carlsbad, CA, USA
40 µm sterile cell strainer	352340		Falcon, Corning	Manassas, VA, USA
FACS buffer	n/a - made in house	0.5% Bovine Serum Albumin, 0.3% Sodium azide in PBS		
Live/dead stain		1:1000	ThermoFisher	Waltham, MA, USA
Fc Receptor Binding Inhibitor		1:50	Invitrogen Corp.	Carlsbad, CA, USA
Rat anti-CD11b antibody APC/Cy7	101225	1:150	Biolegend	San Diego, CA, USA
Tomato Lectin antibody	FL-1171-1		Vectorlabs	Burlingame, CA, USA
IC Fixation buffer	FB001		Invitrogen Corp.	Carlsbad, CA, USA
Goat anti-Iba-1 antibody	ab5076	1:200	Abcam	Cambridge, UK
Donkey anti-goat IgG Antibody Alexa Fluor 488	A-11055	1:100	Invitrogen Corp.	Carlsbad, CA, USA
BD LSR II Flow Cytometer	n/a		BD Biosciences	San Jose, CA, USA
FlowJo software	n/a		BD Biosciences	San Jose, CA, USA
Adult Brain Dissociation Kit for Mouse and Rat	130-107-677		Miltenyi Biotec	Bergisch Gladbach, Germany
Accutase	A1110501		Life Technologies	Waltham, MA, USA
Anti-CD11b MicroBeads	130-126-725		Miltenyi Biotec	Bergisch Gladbach, Germany
IncuCyte pHrodo Bioparticle for Phagocytosis	4616		Essen BioScience, Sartorius	Ann Arbor, MI, USA
BD FACSAria III cell sorter	n/a		BD Biosciences	San Jose, CA, USA
TRIzol	15596026		Invitrogen Corp.	Carlsbad, CA, USA